Development of a high-frequency pulse laser irradiation system for repairing silicon wafers damaged by abrasive machining processes

Jiwang Yan*, Seiya Muto and
Tsunemoto Kuriyagawa

Department of Nanomechanics,
Tohoku University,
Aramaki Aoba 6-6-01, Aoba-ku,
Sendai, 980-8579, Japan
E-mail: yanjw@pm.mech.tohoku.ac.jp
E-mail: muto@pm.mech.tohoku.ac.jp
E-mail: tkuri@m.tains.tohoku.ac.jp
*Corresponding author

Abstract: A four-axis numerically controlled precision stage equipped with a high-frequency nanosecond pulsed Nd:YAG laser system was developed for processing grinding-damaged silicon wafers. The resulting specimens were characterised using a white-light interferometer, a micro-Raman spectroscope and a transmission electron microscope. The results indicate that around the laser beam centre where the laser energy density is sufficiently high, the grinding-induced amorphous silicon was completely transformed into the single-crystal structure. The optimum conditions for one- and two-dimensional overlapping irradiation were experimentally obtained for processing large-diameter silicon wafers. It was found that the energy density level required for completely removing the dislocations is higher than that for recrystallising the amorphous silicon. After laser irradiation, the surface unevenness has been remarkably smoothed.

Keywords: Nd:YAG laser; single crystal silicon; subsurface damage; ultraprecision grinding.

Reference to this paper should be made as follows: Yan, J., Muto, S. and Kuriyagawa, T. (2010) 'Development of a high-frequency pulse laser irradiation system for repairing silicon wafers damaged by abrasive machining processes', *Int. J. Abrasive Technology*, Vol. 3, No. 3, pp.175–189.

Biographical notes: Jiwang Yan is an Associate Professor in the Department of Nanomechanics, Graduate School of Engineering, Tohoku University, Japan. His current research interests include ultraprecision micromachining, optical manufacturing, laser processing of materials, micro/nanomechanics, glass moulding and micro forming.

Seiya Muto is a Masters student in Tohoku University. He is engaged in laser processing of semiconductor wafers.

Tsunemoto Kuriyagawa is a Professor in the Department of Nanomechanics, Graduate School of Engineering, Tohoku University, Japan. His research interests include nanoprecision mechanical fabrication and micro/meso mechanical manufacturing (M4) process.

Copyright © 2010 Inderscience Enterprises Ltd.

Downloaded from Yan Laboratory, Keio University at http://www.yan.mech.keio.ac.jp. Redistribution is subject to copyright licence from the journal publisher.

1 Introduction

Silicon wafers manufactured by mechanical machining processes, such as slicing, cutting, grinding, lapping and polishing, experience subsurface damage like microstructural changes and dislocation defects (Puttick et al., 1994; Shibata et al., 1994; Zarudi and Zhang, 1998; Yan et al., 2009a). The non-destructive measurement (Bismayer et al., 1994; Yan, 2004; Yan et al., 2007a) and the complete removal of subsurface damage from silicon wafers is essential for producing reliable silicon devices. Currently, etching and chemomechanical polishing are two popular methods to remove the subsurface-damaged layer from the bulk material.

An alternative method currently being considered is the use of laser irradiation to realise 'damage repairing'. In a previous paper (Yan et al., 2007b), we demonstrated the feasibility of repairing the lattice structure of a single point diamond-cut silicon wafer by using a nanosecond pulsed Nd:YAG laser which has a pulse frequency of ~50 Hz and a square-shaped beam with uniform energy density. In the present study, in order to realise rapid processing of large-diameter workpieces, a high-frequency nanosecond pulsed Nd:YAG laser repairing system was developed. In this paper, the basic structure and configuration of the developed laser repairing system were introduced briefly first, and then some preliminary experiments were conducted on precision diamond-ground silicon wafers using the developed system. The responses of the workpiece surface microstructure to individual and overlapping laser shots were experimentally investigated and the optimum conditions for overlapping irradiation to process large-diameter silicon wafers were clarified. It is expected that the developed system can be used to post-process large-diameter silicon wafers or infrared lens substrates produced by abrasive machining processes, such as grinding and lapping.

2 Laser repairing mechanism

The laser repairing mechanism of subsurface damages is considered to result from the sudden melting of amorphous silicon and subsequent epitaxial regrowth during cooling. The processing mechanism is schematised in Figure 1. As machining induced amorphous silicon has a remarkably higher absorption coefficient of laser light than crystalline silicon, there will be sufficient absorption of laser in the near-surface layer to form a thin liquid silicon film [Figures 1(a)–1(b)]. The liquid layer is metallic and has a much higher absorption rate, and thus becomes thicker and thicker [Figure 1(c)]. The top-down melted liquid phase finally extends below the deeper dislocated region [Figure 1(d)]. During the period of melting, an initially rough surface becomes a smooth one due to the surface tension effect of the liquid layer [Figure 1(b)–1(d)]. This is similar to the manner in which a free droplet of liquid naturally assumes a spherical shape to achieve a minimum surface area to volume ratio. For a plane wafer, the surface area reaches a minimum when the liquid thin film becomes completely flat at the surface. After the laser pulse, then environmental cooling will result in a bottom-up epitaxial regrowth from the defect-free crystalline region which serves as a seed for crystal growth [Figure 1(e)]. Therefore, by using the material self-organisation phenomena induced by the nanosecond laser pulses, we might be able to achieve both a perfect single-crystal subsurface structure and an extremely smooth surface at the same time [Figure 1(f)].

Figure 1 Schematic model of laser repairing mechanism for abrasive-machined single crystalline materials (see online version for colours)

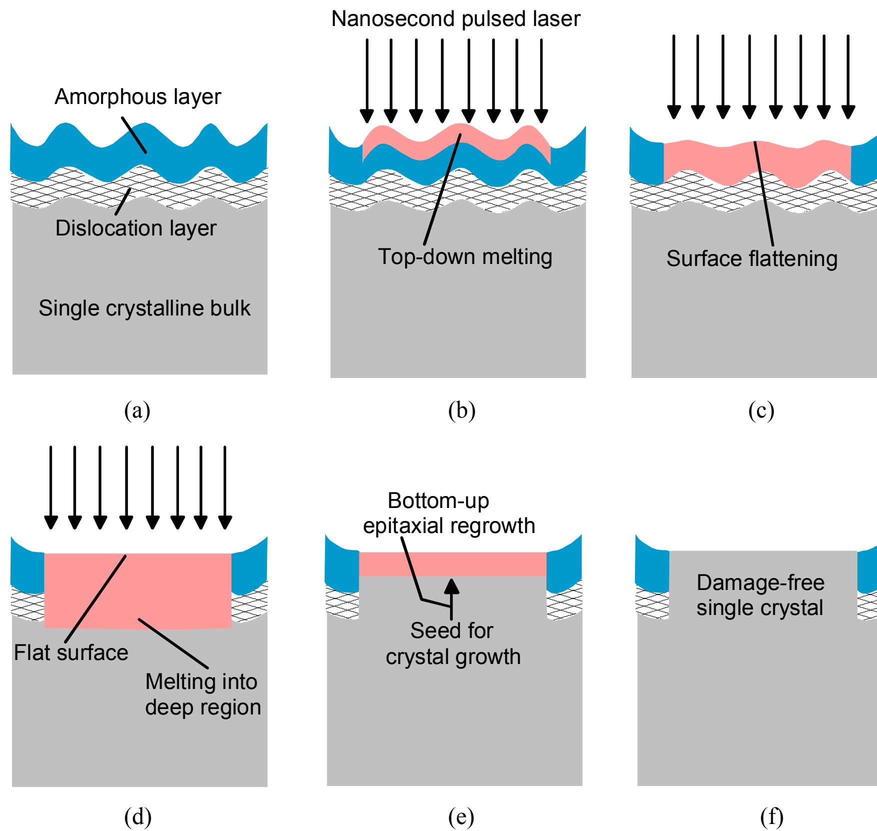

The rapid melting and epitaxial regrowth of silicon in the laser repairing process might be similar to that taking place in the conventional laser annealing processes (Weaire and Wilson, 1978; Lüthy et al., 1979; Boyd and Wilson, 1980; Toet et al., 1997; Andrä et al., 2005), in which amorphous silicon thin films on various substrate materials, such as glass and sapphire, are crystallised by laser irradiation. The major difference between the two processes is that in laser annealing the substrates are non-silicon materials, hence no lattice-matched crystal seed exists. As a result, only poly crystalline structure silicon surfaces can be obtained after laser annealing. In laser repairing, however, the epitaxial crystal regrowth is based on the bulk silicon which has a single crystalline structure. Therefore, the resulting surface will have the same single crystalline structure as the bulk.

Compared with the conventional material removal processes, such as etching and chemomechanical polishing, the proposed laser repairing technique offers a number of advantages:

1 involving no material removal thus preserving the workpiece dimension

2 generating no pollutants

3 enabling selective processing and processing of complex shapes.

3 Experimental setup and procedures

3.1 Experimental setup

A laser-diode exited LR-SHG Nd:YAG laser system (MegaOpto Co., Ltd.) was adopted in this study. The laser has a wavelength of 532 nm. The laser pulse width was 20 ns and the pulse frequency was changeable in a range of 0.1–10 kHz. The output of the laser can be adjusted by the electrical current of the laser diode. The laser output also changes with the pulse frequency. The maximum output was 1 W at a frequency of 1 kHz. The laser beam has a diameter of 600 μm at the window and has a spread angle of 0.2 mrad in air. The energy density profile within the laser beam cross-section follows the Gaussian distribution. The laser beam profile is different from the previously used one (Yan et al., 2007b), which has been shaped into a square (20 μm × 20 μm) within which the energy density is uniform.

Figure 2 (a) Schematic diagram and (b) photograph of the main section of the developed laser repairing system (see online version for colours)

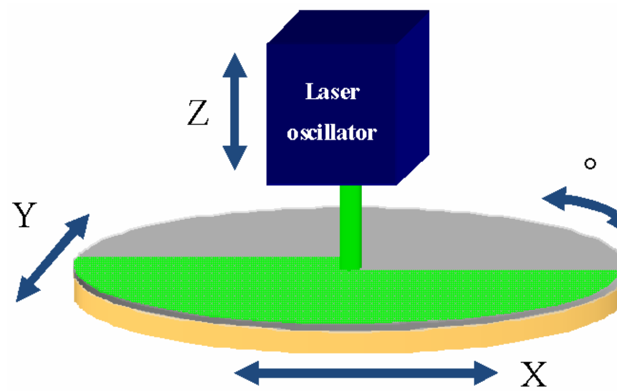

(a)

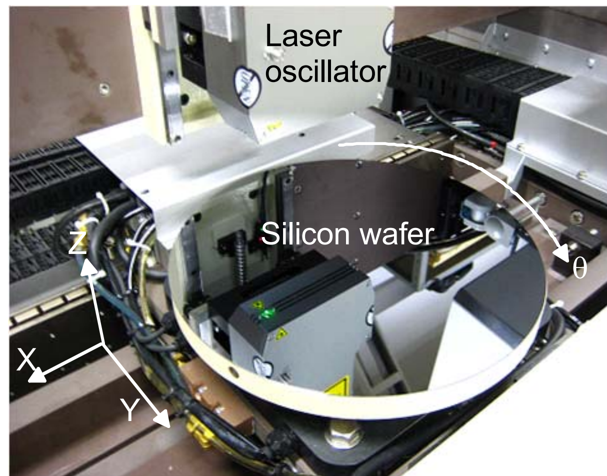

(b)

The laser oscillator was mounted onto a specially developed four-axis (XYZθ) precision stage made of ceramics. The stage is numerically controlled by a personal computer. The laser spot can be directed to the surface of the workpiece which was moved horizontally by XY tables enabling large-area irradiation. The schematic diagram and the photograph of the machine are shown in Figure 2. The XY tables of the stage were driven by linear motors on air slides, enabling a maximum speed of 0.5 m/s. The movement accuracy of the linear tables is ~2 μm within the effective stroke of the tables (420 mm). The movement of XY tables was feedback-controlled by linear scales with a resolution of 0.1 μm. The silicon wafer is vacuum-chucked on a rotary table which can rotate along the θ axis on the XY tables at a speed of 180 rpm. The rotary table has a diameter of 300 mm. The rotary table and the vacuum chuck were also made of ceramics and supported by precision ball bearings, enabling a run out of ~10 μm.

This system was designed to be capable of processing both flat surfaces and curved surfaces, such as aspherical silicon lenses, as well as partially selective processing of a workpiece. In this paper, we name the developed system as the 'laser irradiation surface creator (LISC)'. Table 1 shows the main specifications of the system. In the experiments of the present paper, the spacing between adjacent laser irradiations was adjusted by changing the speed of the XY tables of the stage while keeping the laser frequency unchanged.

Table 1 System specifications

Laser oscillator	
Wavelength	532 nm
Pulse width	20 ns
Pulse frequency	0.1–10 kHz
Excitation	Laser diode
Maximum output	1 W
Beam diameter	600 μm
Beam profile	Gaussian distribution
Supporting stage	
Freedom of movement	Four-axis (XYZθ)
Stage material	Ceramics
Movement accuracy	~2 μm
Stepping resolution	0.1 μm
Maximum speed	0.5 m/s
Strokes	420 mm
Diameter of rotary table	300 mm

3.2 Sample preparation

Electric device-grade p-type single-crystal silicon (100) wafers produced by diamond grinding were used as specimens. Diamond grinding was carried out using an ultraprecision grinder equipped with vitrified grinding wheels with fine diamond abrasives. The average size of the abrasive grains was approximately 2 μm.

3.3 Surface characterisation

The surface topography of the silicon wafer was examined by a white-light interferometer NewView 5000 (Zygo Corporation) before and after later irradiation. A micro-Raman spectrometer (NRS-3100, JASCO Corporation) was used to characterise the microstructural changes of the samples. The wavelength of the laser used for the Raman spectroscopy was 532 nm, and the focused laser spot size was 1 μm in diameter. The laser exposure time was 1 second. Also, cross-sectional observations of the samples were performed with a transmission electron microscope (TEM) HF2000 (Hitachi Ltd.) where the acceleration voltage used was 200 kV.

Figure 3 Energy density distributions of the laser beam at: (a) various electrical currents at a fixed distance of 30 mm from the window (b) various distances at a constant electrical current of 30 A (see online version for colours)

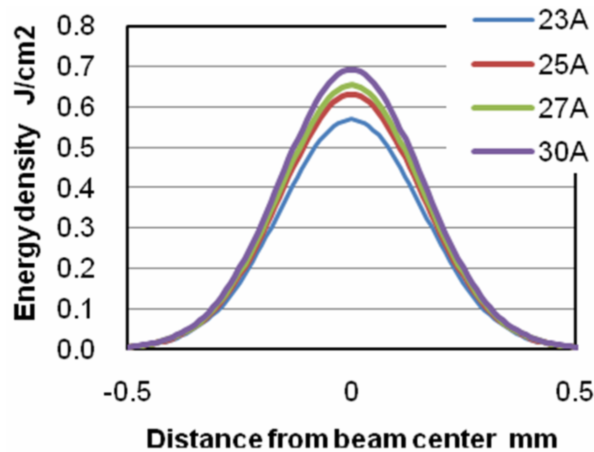

(a)

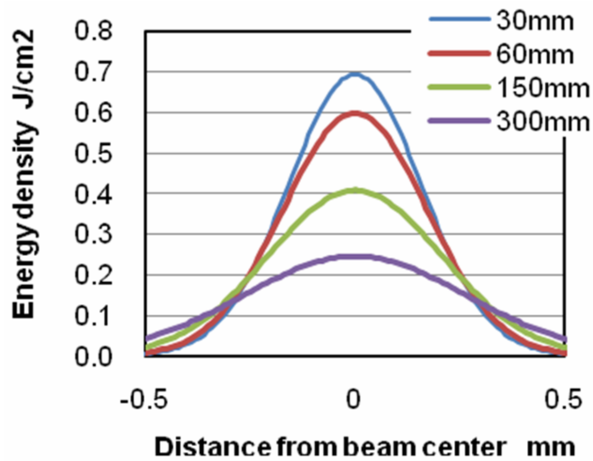

(b)

4 Results and discussion

4.1 Measurements of laser energy density profiles

In this study, the energy density profile of the laser beam is not uniform but follows the Gaussian distribution. To quantitatively characterise the energy density distribution, the laser beam profile was measured by a BeamView Analyzer (Coherent Japan Inc.) and the energy of per laser pulse was measured by a laser power meter. The energy density $E(r)$ at a distance r from the beam centre can be described by:

$$E(r) = \frac{8E_0}{\pi d^2} \exp\left(-\frac{8r^2}{d^2}\right) \tag{1}$$

where d is the beam diameter and E_0 is the pulse energy. Figure 3 shows calculation results of energy density distribution at a pulse frequency of 500 Hz. In Figure 3(a), the beam profile was measured at a distance of 30 mm from the laser beam window at various electrical currents of the exciting laser diode. It can be seen that the energy density increases with the electrical current while the laser beam diameter does not change. The measurement in Figure 3(b) was performed at various distances from the laser beam window at a fixed electrical current of 30 A. It is evident that as the distance increases, the energy density decreases but the laser beam diameter increases.

4.2 Single-pulse irradiation

To begin with, single-pulse laser irradiations were performed on the silicon wafers. By moving the X table of the stage at a speed of 0.3 m/s at a laser pulse frequency of 500 Hz, individual laser shots with a spacing of 600 μm were obtained. After laser irradiation, the sample surface was observed using a microscope. Figure 4 shows micrographs of the laser-irradiated surfaces at pulse energy levels of 0.6 and 1.0 J, respectively. It can be seen that there is a slight change in contrast between the irradiated region and the unirradiated region and the area of the dark region increases with the pulse energy. As known from the Raman spectroscopy, which will be shown later, the dark regions are the phase-transformed regions caused by laser irradiation.

Next, laser micro-Raman spectroscopy was used to examine the phase transformation of silicon. Figures 5(a)–5(d) show typical Raman spectra of the unirradiated point A and the irradiated points B, C and D, respectively, as indicated in Figure 4(b). At point A [Figure 5(a)], a strong Raman response around 470 cm^{-1} is seen, indicating presence of amorphous silicon (*a*-Si). At point B [Figure 5(b)], the Raman spectrum is very similar to that in Figure 5(a), indicating that the energy density at this point is too low to cause crystallisation of the amorphous silicon. At point C [Figure 5(c)], the Raman intensity at 470 cm^{-1} has become considerably smaller, but is still higher than the baseline. This result indicates that crystallisation of amorphous silicon has taken place but the crystallisation was not complete. At point D [Figure 5(d)], the Raman intensity at 470 cm^{-1} is completely the same as the baseline, indicating that under this energy density level the amorphous silicon phase has been completely transformed into single crystalline silicon.

Figure 4 Micrographs of laser irradiated surfaces at different levels of pulse energy, (a) 0.6 J (b) 1 J (see online version for colours)

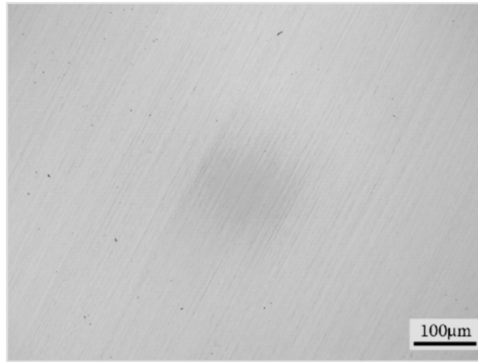

(a)

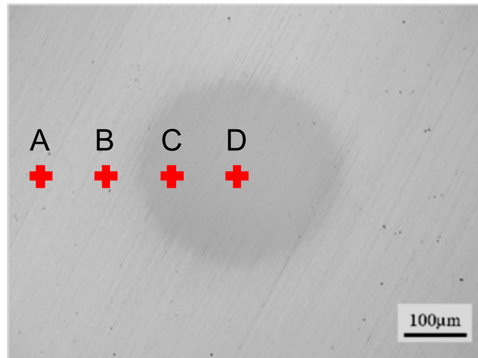

(b)

Figure 5 Raman spectra of the diamond ground silicon wafer, (a) unirradiated region A (b)–(d) corresponding to the laser irradiated points B–D as indicated in Figure 4(b) (see online version for colours)

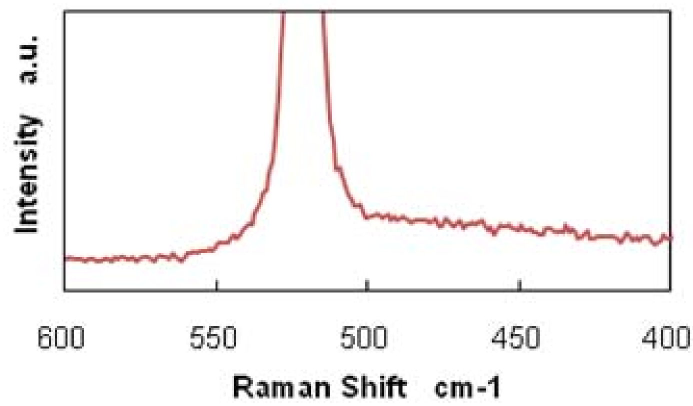

(a)

Figure 5 Raman spectra of the diamond ground silicon wafer, (a) unirradiated region A (b)–(d) corresponding to the laser irradiated points B–D as indicated in Figure 4(b) (continued) (see online version for colours)

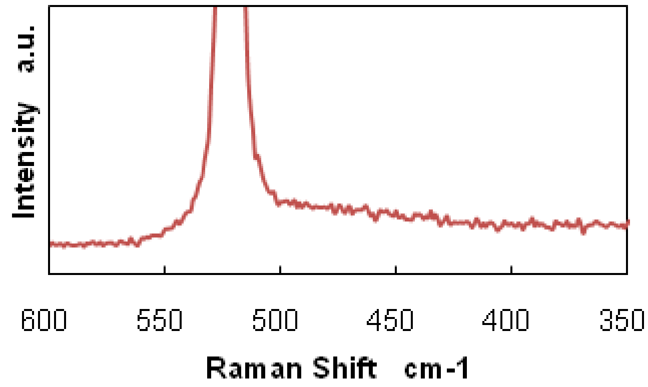

(b)

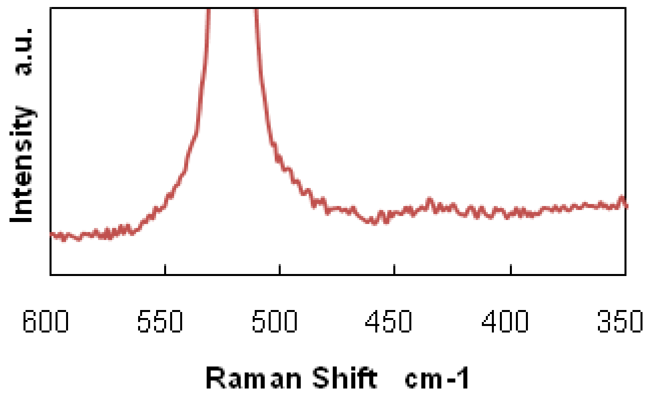

(c)

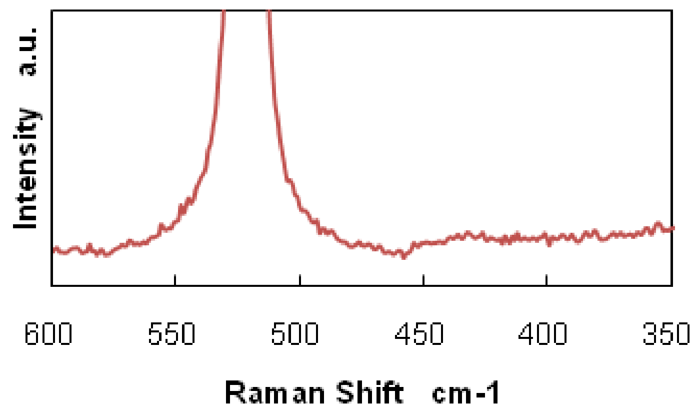

(d)

To quantitatively characterise the subsurface microstructural changes of silicon, we introduced a new parameter, namely Raman intensity ratio *r*, which is defined by:

$$r = \frac{A_{515-525}}{A_{515-525} + A_{350-515}} \quad (2)$$

where $A_{515-525}$ is the area integration of the Raman spectra in a range of 515–525 cm^{-1} which corresponds to single crystalline silicon; $A_{350-515}$ is the integration of the Raman spectra in a range of 350–515 cm^{-1} which corresponds to amorphous and polycrystalline silicon. Hence, the bigger the Raman intensity ratio *r* is, the stronger the single crystallinity is. By calibration using thermally annealed silicon wafers, it was found that a silicon wafer with no amorphous layer yield a value of *r* bigger than 0.85. Figure 6 is a plot of the Raman intensity ratio of the laser irradiated region in Figure 4(b). It can be seen that near the laser beam centre the curve tends to be flat where $r > 0.85$. This region, the diameter of which is approximately 250 μm, is the crystallised region after laser irradiation. By comparing the curve in Figure 6 with the energy density curve in Figure 3(a), it is found that the critical energy density for completely recrystallise the amorphous silicon is 0.48 J/cm^2. This critical value is an important guideline for overlapping irradiation which will be discussed in the next session.

Figure 6 Plot of Raman intensity ratio cross the laser irradiated region shown in Figure 4(b) (see online version for colours)

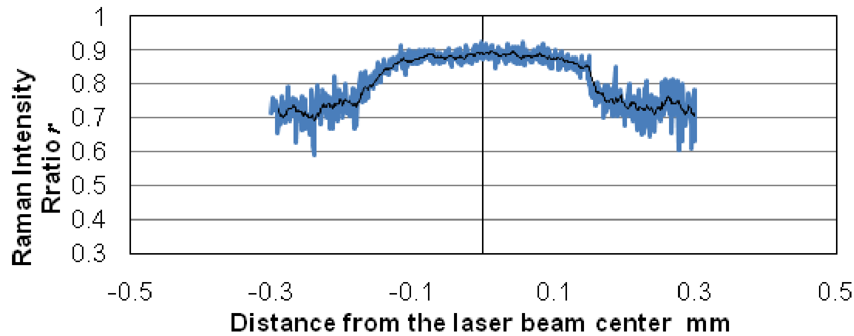

4.3 Overlapping irradiation

To recover the subsurface damage of a large-diameter silicon wafer, it is necessary to scan the laser beam across the wafer so as to overlap successive irradiation runs. Perfect crystallinity at the boundary among adjacent irradiations is essential for guaranteeing the subsurface integrity of the entire wafer [5]. For this purpose, the design of the scanning path of the laser beam on the wafer is an important step. The laser scanning path should meet two requirements: one is that the energy density over the entire wafer must be higher than the critical value (0.48 J/cm^2); the other is that the processing speed must be as high as possible.

Figure 7 Plots of Raman intensity ratio of overlapping irradiated wafer at various spaces, (a) 350 μm, (b) 250 μm (see online version for colours)

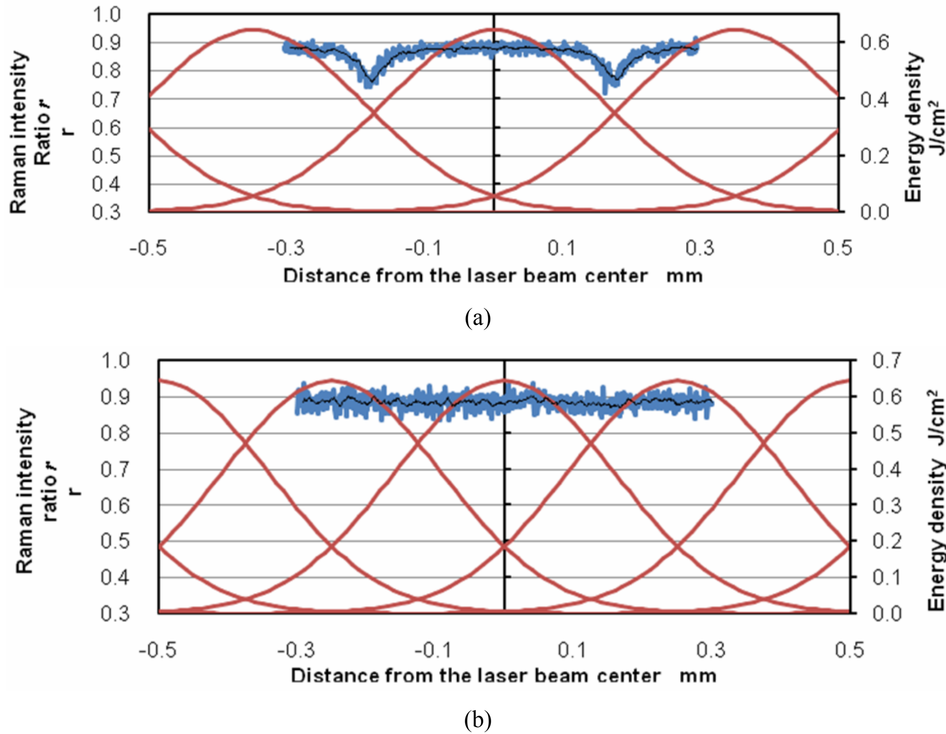

(a)

(b)

Figure 7 shows plots of Raman intensity ratio of one-dimensionally overlapped irradiations at different spaces, 350 and 250 μm. The Raman intensity measurements were performed along the line passing through the laser irradiation centres. In the figure, the corresponding energy density profiles were also shown. In Figure 7(a), there are remarkable depressions on the Raman intensity ratio curve between adjacent laser shots, indicating that the overlap spacing is too large to achieve complete subsurface reconstruction. In Figure 7(b), however, the curve tends to be very flat ($r > 0.85$), demonstrating that the overlapping spacing under this condition is small enough to achieve a continuous single crystalline surface.

Next, two-dimensional overlapping irradiation was performed. Figure 8 shows two examples of Raman intensity ratio mapping after laser irradiation at different spaces. Figure 8(a) is obtained at a space of 150 μm in X direction and a space of 300 μm in Y direction. In this case, the Y spacing is so big that residual amorphous region can be clearly seen. Figure 8(b) is obtained at a space of 200 μm in both X and Y directions. In this case, the maximum distance between any two adjacent laser irradiations is smaller than the critical value (250 μm), so that the amorphous silicon on the entire wafer surface has been completely transformed into a crystalline structure.

Figure 8 Raman intensity ratio mapping results after laser irradiation at spaces of (a) 150:300 (b) 200:200 µm (see online version for colours)

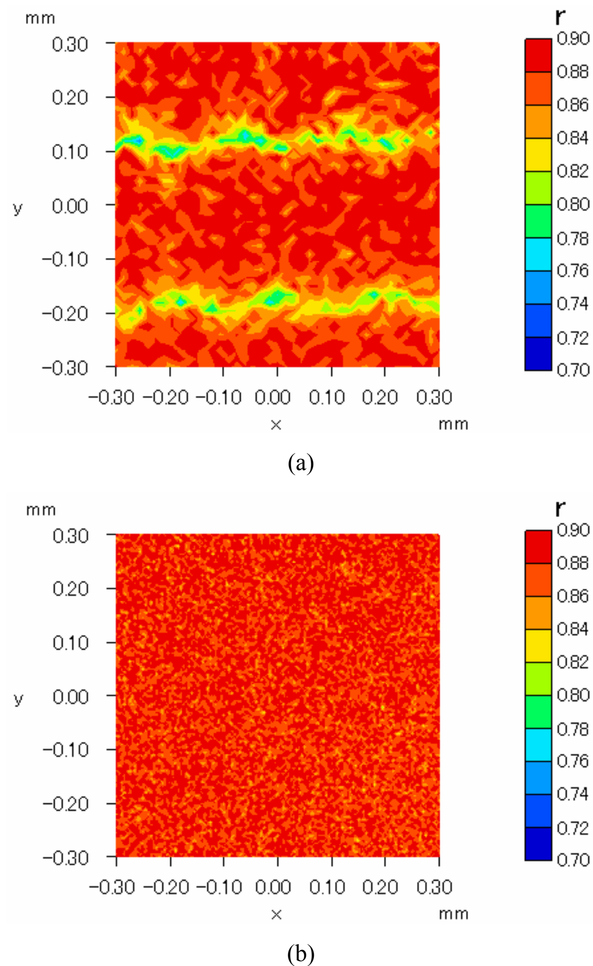

(a)

(b)

4.4 *TEM observation of subsurface microstructures*

Figure 9(a) shows a cross-sectional TEM micrograph of a diamond-ground silicon wafer before laser irradiation. It is clear that the ground surface is far from being flat but has waviness in the size scale of a few tens of nanometres. Below the ground surface, there is a non-uniform grey layer (grinding-induced amorphous layer). Beneath the amorphous layer, there are dislocations. Figure 9(b) is a cross-sectional TEM photograph of the laser irradiated region at a spacing of 200:200 µm (X:Y). The amorphous layer has completely disappeared, indicating the recrystallisation of silicon was performed successfully. However, there are still a few residual dislocations. Figure 9(c) is a TEM photograph of the laser irradiated region at a much smaller spacing of 100:100 µm (X:Y). The minimum laser energy density in this case was 0.63 J/cm^2. It is clear that both the grey layer and the dislocations have completely disappeared and a perfect single crystalline structure identical to that of the bulk material has been achieved. This result is very similar to that

obtained by the square-shaped laser beam which has uniform energy density, where excellent subsurface microstructural uniformity was achieved in overlapping laser irradiation without forming crystalline grain boundaries (Yan et al., 2009b).

Figure 9 Cross-sectional TEM micrographs of silicon wafers: (a) before laser irradiation and after laser irradiation at two-dimensional spacing of (b) 200 μm and (c) 100 μm

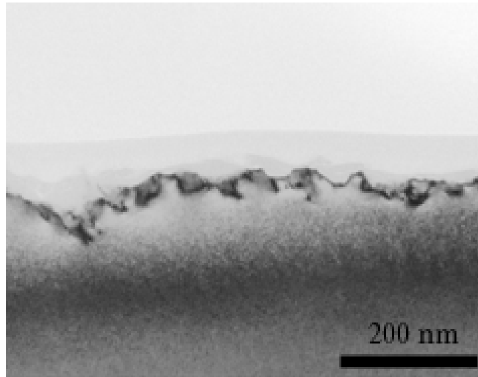

(a)

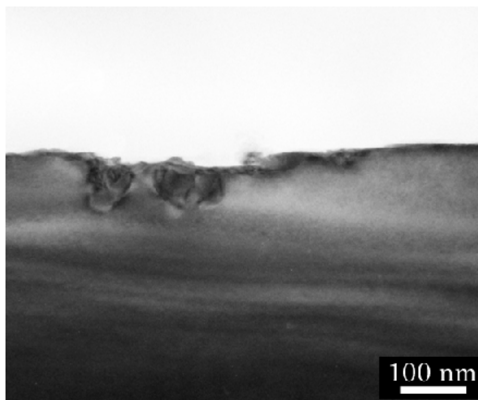

(b)

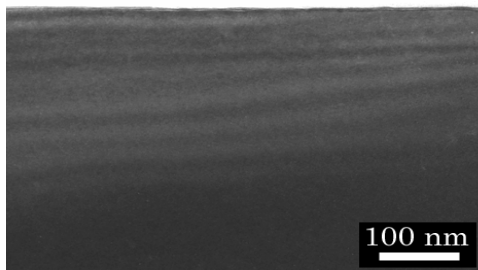

(c)

From the above results, we can say that a sufficient laser energy density level is essential to achieve complete recovery of grinding damages, and that the laser energy density required for repairing dislocations is higher than that for recrystallising the amorphous silicon. After laser irradiation, the surface flatness has also been significantly improved. The grinding-induced unevenness on the surface has been successfully smoothed.

5 Conclusions

A high-frequency nanosecond pulsed laser irradiation system was developed for repairing silicon wafers having subsurface damage formed in ultraprecision diamond grinding. The preliminary experimental results indicate that around the laser beam centre where the laser energy density is sufficiently high, the grinding-induced amorphous silicon was completely transformed into the single-crystal structure. The optimum conditions for one- and two-dimensional overlapping irradiation were experimentally obtained for processing large-diameter silicon wafers. It was found that the energy density level required for completely removing the dislocations is much higher than that for recrystallising the amorphous silicon. After laser irradiation, surface unevenness has been significantly smoothed.

Acknowledgements

We would like to thank Covalent Materials Corporation for providing silicon wafers and related technical information. This work has been supported by a Grant-in-Aid for Exploratory Research (Project No. 20656023) from the Japan Society for the Promotion of Science (JSPS).

References

Andrä, G., Bergmann, J. and Falk, F. (2005) 'Laser crystallized multicrystalline silicon thin films on glass', *Thin Solid Films*, Vol. 487, Nos. 1–2, pp.77–80.

Bismayer, U., Brinksmeier, E., Güttler, B., Seibt, H. and Menz, C. (1994) 'Measurement of subsurface damage in silicon wafers', *Precision Engineering*, Vol. 16, No. 2, pp.139–144.

Boyd, I.W. and Wilson, J.I.B. (1980) 'Laser annealing for semiconductor devices', *Nature*, Vol. 287, pp.278–278.

Lüthy, W., Affolter, K., Weber, H.P., Roulet, M.E., Fallavier, M., Thomas, J.P. and Mackowski, J. (1979) 'Dynamics of Nd:YAG laser annealing of silicon on sapphire', *Applied Physics Letter*, Vol. 35, pp.873–875.

Puttick, K.E., Whitmore, L.C., Chao, C.L. and Gee, A.E. (1994) 'Transmission electron microscopy of nanomachined silicon crystals', *Philosophical Magazine A*, Vol. 69, No. 1, pp.91–103.

Shibata, T., Ono, A., Kurihara, K., Makino, E. and Ikeda, M. (1994) 'Cross-section transmission electron microscope observations of diamond-turned single-crystal Si surfaces', *Applied Physics Letter*, Vol. 65, No. 20, pp.2553–2555.

Toet, D., Koopmans, B., Bergmann, R.B., Richards, B., Santos, P.V., Albrecht, M. and Krinke, J. (1997) 'Large area polycrystalline silicon thin films grown by laser-induced nucleation and solid phase crystallization', *Thin Solid Films*, Vol. 296, Nos. 1–2, pp.49–52.

Weaire, D. and Wilson, J.I.B. (1978) 'Laser annealing of semiconductors', *Nature*, Vol. 276, pp.668–669.

Yan, J. (2004) 'Laser micro-Raman spectroscopy of single-point diamond machined silicon substrates', *Journal of Applied Physics*, Vol. 95, No. 4, pp.2094–2101.

Yan, J., Asami, T. and Kuriyagawa, T. (2007a) 'Nondestructive measurement of machining-induced amorphous layers in single-crystal silicon by laser micro-Raman spectroscopy', *Precision Engineering*, Vol. 32, pp.186–195.

Yan, J., Asami, T. and Kuriyagawa, T. (2007b) 'Response of machining-damaged single-crystalline silicon wafers to nanosecond pulsed laser irradiation', *Semiconductor Science and Technology*, Vol. 22, pp.392–395.

Yan, J., Asami, T. and Kuriyagawa, T. (2009b) 'Complete recovery of subsurface structures of machining-damaged single crystalline silicon by Nd:YAG laser irradiation', *Key Engineering Materials*, Vol. 389–390, pp.469–474.

Yan, J., Asami, T., Harada, H. and Kuriyagawa, T. (2009a) 'Fundamental investigation of subsurface damage in single crystalline silicon caused by diamond machining', *Precision Engineering*, Vol. 33, No. 4, pp.378–386.

Zarudi, I. and Zhang, L.C. (1998) 'Effect of ultraprecision grinding on the microstructural change in silicon monocrystals', *Journal of Materials Processing Technology*, Vol. 84, pp.149–158.